Preprints (www.preprints.org) | NOT PEER-REVIEWED | Posted: 28 December 2021 doi:10.20944/preprints202112.0443.v1

Article

Assessing the Potential of Multi-spectral and Multi-temporal Satellite Images for Classification and Mapping of Plant Communities in a Temperate Region

Ram C. Sharma[1]*, Hidetake Hirayama[1], Masatsugu Yasuda[2], Itsuki Asai[2] and Keitarou Hara[1]

[1] Department of Informatics, Tokyo University of Information Sciences, 4-1 Onaridai, Wakaba-ku, Chiba 265 8501, Japan; sharma@rsch.tuis.ac.jp, hh207501@rsch.tuis.ac.jp, hara@rsch.tuis.ac.jp
[2] Asia Air Survey Co., Ltd., Kawasaki City, Kanagawa, Japan; mtg.yasuda@ajiko.co.jp, mk.asai@ajiko.co.jp
*Correspondence: ram-c-sha@pm.me; Tel.: +81-43-236-4603.

Abstract: Classification and mapping of plant communities is an essential step for conservation and management of ecosystems and biodiversity. We adopt the Genus-Physiognomy-Ecosystem (GPE) system developed in previous study for satellite-based classification of plant communities. This paper assesses the potential of multi-spectral and multi-temporal images collected by Sentinel-2 satellites. This research was conducted in five representative study sites in a temperate region. It consists of 44 types of plant communities including a few land cover types as well. The plant community types were enumerated in the study sites and ground truth data were prepared with reference to extant vegetation surveys, visual interpretation of high-resolution images, and onsite field observations. We acquired all Sentinel-2 Level-1C product images available for the study sites between 2017-2019 and generated monthly median composite images consisting of ten spectral and twelve spectral-indices. Gradient Boosting Decision Trees (GBDT) classifier was employed as an efficient and distributed gradient boosting technique for the supervised classification of big datasets involved in the research. The cross-validation accuracy in terms of kappa coefficient varied from 87% in Oze site with 41 land cover and plant community types to 95% in Hakkoda site with 19 land cover and plant community types; with average performance of 91% across all sites. In addition, the resulting maps demonstrated a clear distribution of plant community types involved in all sites, highlighting the potential of Sentinel-2 multi-spectral and multi-temporal images with GPE classification system for operational and broad-scale mapping of land cover and plant communities.

Keywords: Sentinel-2, Land cover, Vegetation, Mapping, Plant communities, Machine learning, Genus-Physiognomy-Ecosystem, Gradient Boosting Decision Trees

1. Introduction

Classification and mapping of plant communities is an essential step for conservation and management of ecosystems and biodiversity. In recent years, availability of free and open access data, high performance computing, and automated data processing and analysis capabilities have brought new opportunities for classification and mapping of plant communities from remotely sensed images (Murakami and Mochizuki, 2014; Wulder, 2018). In contrast to potential natural vegetation mapping based on climatic

Preprints (www.preprints.org) | NOT PEER-REVIEWED | Posted: 28 December 2021 doi:10.20944/preprints202112.0443.v1

parameters available at coarse spatial resolution (Hengl et al., 2018), actual vegetation mapping (Bredenkamp et al., 1998; Su et al., 2020) with recently available satellite images can provide much detailed information at higher spatial resolution for improving the knowledge of plant community.

In Japan, a wide variety of land cover and plant communities, ranging from Southern Subtropical Forests to Northern Arctic Meadows, exists (Numata et al., 1972; Miyawaki, 1984; Himiyama, 1998). Nationwide vegetation surveys have been conducted continuously since 1973 and distribution of plant communities is well known. First vegetation survey of the entire country was completed in 1999 with the production of vegetation survey maps at 1:50,000 scale (MoE and AAS, 1999). Since 1999, extensive field surveys have been repeated and a 1:25,000 scale vegetation survey map is being produced nationwide (Hioki, 2007). The vegetation survey follows phyto-sociological units based organization plant communities (Miyawaki 1968; Ohno, 2006). The plant communities are recognized through field surveys and delineated in a geographical environment via a manual procedure facilitated by visual interpretation of aerial and satellite images. The manual delineation procedure is subject to human discernment, laborious, and costly. To cope with these issues, more intelligent technology has been expected.

The major objective of this paper is to assess the potential of multi-spectral and multi-temporal images available from the Sentinel-2 mission satellites (Sentinel-2A and 2B) for operational and broad-scale mapping of land cover and plant community types by adopting the Genus-Physiognomy-Ecosystem (GPE) system developed in previous study for satellite-based classification of plant communities.

2. Materials and Methods

2.1. Study sites

This research was conducted in five representative sites of the Tohoku region in Japan. These five study sites were selected in such a way that they can represent all land cover and plant communities types present in the Tohoku region. The location map of five study sites has been shown in Figure 1.

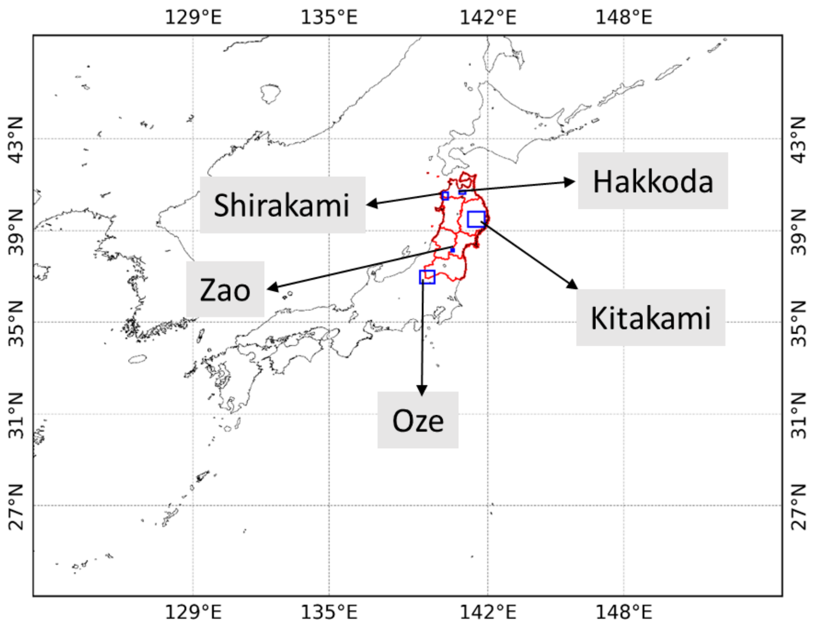

Figure 1. The location of five study sites (Hakkoda, Oze, Zao, Shirakami, and Kitakami) are shown by blue rectangles in the Tohoku region of Japan (red polygon).

Preprints (www.preprints.org) | NOT PEER-REVIEWED | Posted: 28 December 2021 doi:10.20944/preprints202112.0443.v1

2.2. Preparation of ground truth data

First of all, land cover and plant community types present in five study sites were enumerated by adopting the Genus-Physiognomy-Ecosystem (GPE) system developed in previous study (Sharma, 2021) for satellite-based classification and mapping of plant communities. Extant vegetation survey reports available from Nature Conservation Bureau, Ministry of the Environment and Asia Air Survey Co., Ltd were utilized as reference materials for enumerating land cover and plant community types in each study site. The land cover and plant community types were further verified by onsite field observations conducted between 2017 and 2020 in all study sites. The final confirmed list of land cover and plant community types present in five study sites has been described in Table 1.

Table 1. List of land cover and plant community types of Tohoku region enumerated in the research. The occurrence of land cover and plant community types in each study site are denoted by asterisk (*) symbol.

Classes	Hakkoda	Oze	Zao	Shirakami	Kitakami
Abies ECF	*	*	*		*
Acer DBF		*	*		
Alnus DBF	*	*	*		*
Alpine Herb		*	*	*	*
Alpine Shrub			*		*
Bamboo EBF		*			*
Barren	*	*	*	*	*
Betula DBF	*	*	*	*	*
Carpinus DBF		*		*	*
Cryptomeria ECF	*	*	*	*	*
Euptelea DBF		*			
Fagus DBF	*	*	*	*	*
Fraxinus DBF		*		*	*
Hydrangea Shrub		*	*		
Juglans DBF		*		*	*
Larix DCF	*	*	*	*	*
Miscanthus Herb	*	*	*	*	*
Other Herb	*	*	*	*	
Other Shrub	*	*	*		*
Paddy field		*		*	*
Pasture	*	*		*	*
Picea ECF					*
Pinus ECF	*	*	*	*	*
Pinus Shrub	*	*	*	*	*
Populus DBF		*			
Pterocarya DBF	*	*	*	*	*
Quercus DBF	*	*	*	*	*

Quercus Shrub	*	*	*	*	
Rhododendron Shrub		*			*
Robinia DBF		*		*	*
Salix DBF		*		*	*
Salix Shrub		*	*	*	*
Sasa Shrub	*	*	*	*	*
Thuja ECF		*			
Thujopsis ECF		*			*
Tsuga ECF	*	*	*		*
Ulmus DBF		*			*
Upland field		*		*	*
Urban builtup		*	*	*	*
Water		*	*	*	*
Wetland Herb	*	*	*		*
Zanthoxylum DBF		*			
Zelkova DBF		*		*	*
Zoysia Herb					*
Total classes	19	41	25	26	36

DBF: Deciduous Broadleaf Forest; DCF: Deciduous Conifer Forest
ECF: Evergreen Conifer Forest; EBF: Evergreen Broadleaf Forest

The ground truth data, polygons representing homogeneous land cover and plant community types of around 1ha size, were collected with reference to extant vegetation survey maps (1:25,0000 scale) produced from extensive field surveys between 2012 to 2020, and visual interpretation of time-lapse images available in the Google Earth by local experts in plant ecology and vegetation sciences. The distribution of ground truth data in the study sites has been shown in Figure 2.

Preprints (www.preprints.org) | NOT PEER-REVIEWED | Posted: 28 December 2021 doi:10.20944/preprints202112.0443.v1

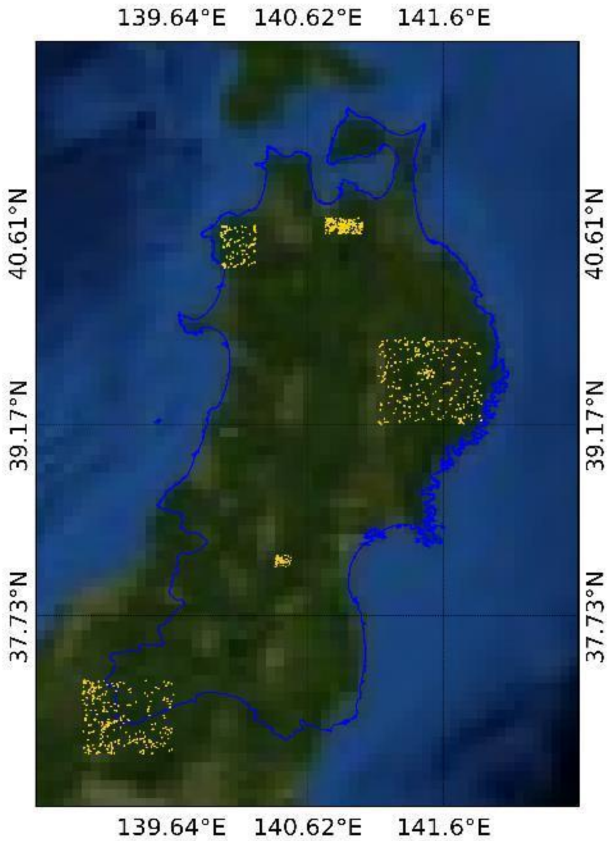

Figure 2. The distribution of ground truth data (yellow color) collected in the research.

2.3. Processing of satellite data

We acquired all Level-1C product images collected by Sentinel-2 mission satellites (Sentinel-2A and 2B) for the study sites between 2017-2019. The Sentinel-2 mission satellites collect optical imagery at high spatial resolution (10-60m) in visible, near infrared, and short-wave wavelengths at a frequency of five days (Drusch et al., 2012). The images were processed for cloud masking and ten spectral bands (blue, green, red, red edge 1-3, near infrared, mid infrared, and shortwave infrared 1-2) were extracted. For each scene, twelve vegetation indices (as shown in Table 2) were also calculated. The spectral and spectral-indices images were composited by computing monthly median values. In this manner, we generated 264 features (22 spectral and spectral-indices × 12 months) altogether for machine learning, classification, and mapping.

Table 2. List of vegetation indices utilized in the research. Blue (B, Band 2), Green (G, Band 3), Red (R, Band 4), Red edge1 (RE1, Band 5), Red edge3 (RE3, Band 7), and Near infrared (N, Band 8) were used for calculating the vegetation indices.

Spectral indices	Formula	References
Atmospherically Resistant Vegetation Index (ARVI)	$\frac{N-R-(R-B)}{N+R-(R-B)}$	Kaufman and Tanre, 1992
Enhanced Vegetation Index (EVI)	$2.5\times\frac{N-R}{(N+6\times R-7.5\times B)+1}$	Huete et al., 2002
Green Atmospherically Resistant Index (GARI)	$\frac{N-(G-1.7\ \times(B-R))}{N+(\ G-1.7\ \times(B-R))}$	Gitelson et al., 1996
Green Leaf Index (GLI)	$\frac{(G-R)+(G-B)}{(2*G)+R+B}$	Louhaichi et al., 2001
Green Red Vegetation Index (GRVI)	$\frac{G-R}{G+R}$	Falkowski et al., 2005
Modified Red Edge Simple Ratio (MRESR)	$\frac{RE3-B}{RE1-B}$	Sims and Gamon, 2002
Modified Soil Adjusted Vegetation Index (MSAVI)	$\frac{2N+1-\sqrt{(2N+1)^2-8(N-R)}}{2}$	Qi et al., 1994
Normalized Difference Vegetation Index (NDVI)	$\frac{N-R}{N+R}$	Rouse et al., 1974
Optimized Soil Adjusted Vegetation Index (OSAVI)	$\frac{(N-R)}{(N+R+0.16)}$	Rondeaux et al., 1996
Red Edge Normalized Difference Vegetation Index (RENDVI)	$\frac{RE3-RE1}{RE3+RE1}$	Gitelson and Merzlyak, 2003
Soil-Adjusted Vegetation Index (SAVI)	$\frac{1.5\ \times(N-R)}{N+R+0.5}$	Huete, 1988
Structure Insensitive Pigment Index (SIPI)	$\frac{N-B}{N-R}$	Penuelas et al., 1995

2.4. Machine learning and classification

We employed Gradient Boosting Decision Trees (GBDT) classifier implemented by XGBoost, an efficient and optimized distributed gradient boosting library (https://github.com/dmlc/xgboost) for the supervised classification of Sentinel-2 images as it can handle large data volume with Compute Unified Device Architecture (CUDA) computations. We implemented a train-test split method for fine tuning of input features and model parameters. Classification accuracy metrics (Accuracy, Kappa coefficient, F1-score, Recall, and Precision) were utilized for quantitative evaluation. For this method, ground truth data were shuffled and randomly splitted into train (75%) and test (25%) sets. The GBDT model was trained on the training data, whereas test data was utilized for fine tuning the parameters of the model. The GBDT model established in this was utilized for prediction and mapping of land cover and plant community types separately for each site.

3. Results and Discussion

3.1. Model test results

The model test results obtained from the machine learning (GBDT classifier) of multi-temporal Sentinel-2 images have been shown using the confusion matrix figures (Figures 3-5) for three sites (Hakkoda, Zao, and Shirakami). Due to many classes involved, class-wise accuracy tables (Tables 3 and 4) have been shown for two sites (Oze and Kitakami).

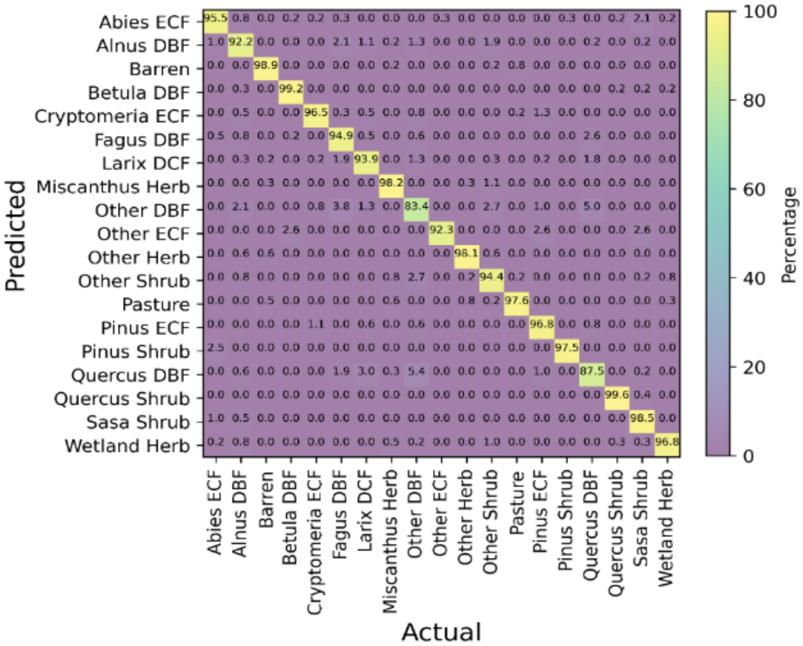

Figure 3. Confusion matrix obtained for Hakkoda site.

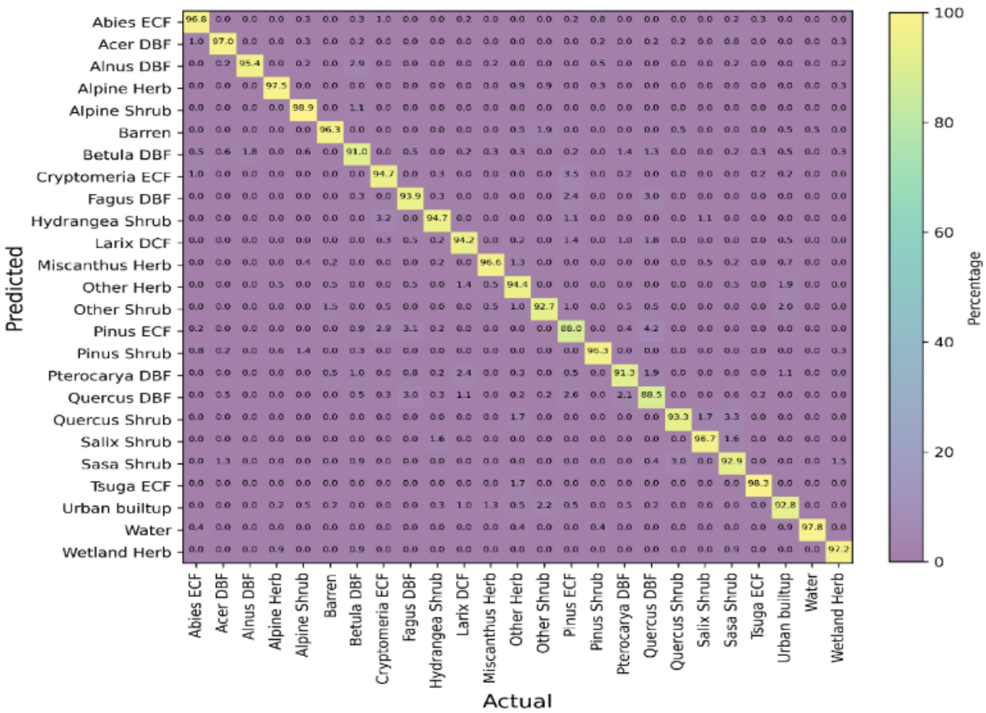

Figure 4. Confusion matrix obtained for Zao site.

Preprints (www.preprints.org) | NOT PEER-REVIEWED | Posted: 28 December 2021 doi:10.20944/preprints202112.0443.v1

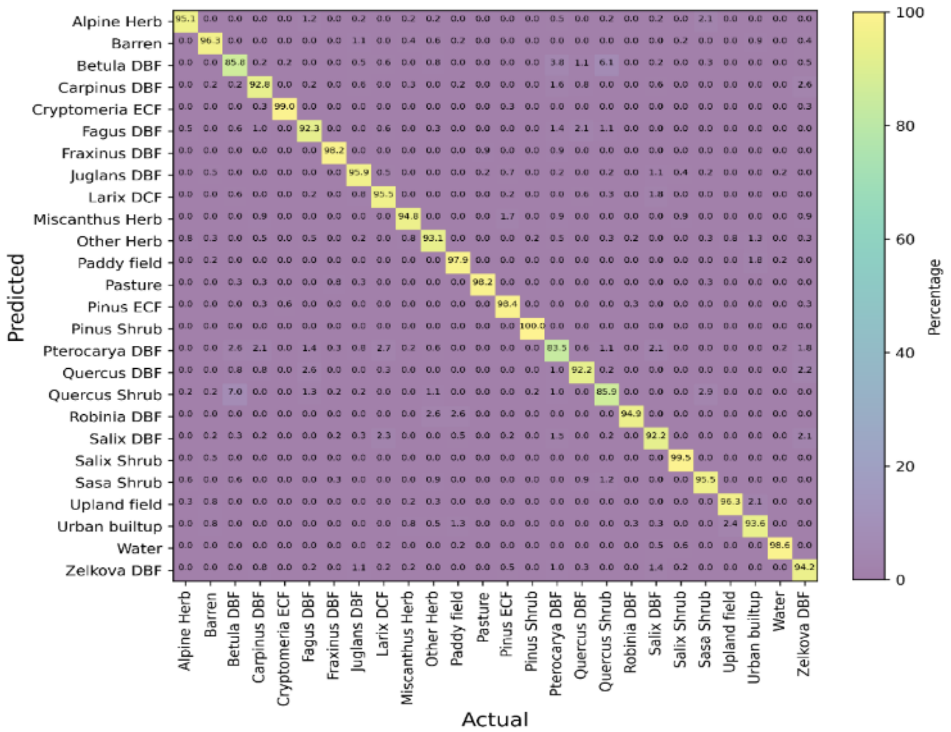

Figure 5. Confusion matrix obtained for Shirakami site.

Table 3. Class-wise accuracy obtained for Oze site.

Classes	Accuracy	Kappa	F1-score	Recall	Precision
Abies ECF	0.995	0.891	0.955	0.84	0.894
Acer DBF	0.996	0.927	0.915	0.944	0.929
Alnus DBF	0.986	0.716	0.736	0.712	0.724
Alpine Herb	0.996	0.927	0.921	0.936	0.929
Bamboo EBF	1.000	1.000	1.000	1.000	1.000
Barren	0.994	0.890	0.883	0.904	0.893
Betula DBF	0.988	0.766	0.785	0.760	0.772
Carpinus DBF	0.995	0.904	0.885	0.928	0.906
Cryptomeria ECF	0.991	0.820	0.861	0.792	0.825
Euptelea DBF	0.994	0.882	0.875	0.896	0.885
Fagus DBF	0.987	0.760	0.723	0.816	0.767
Fraxinus DBF	0.998	0.968	0.947	0.992	0.969
Hydrangea Shrub	0.985	0.718	0.701	0.752	0.726
Juglans DBF	0.991	0.832	0.797	0.88	0.837
Larix DCF	0.994	0.877	0.914	0.848	0.880
Miscanthus Herb	0.993	0.870	0.866	0.88	0.873
Other Herb	0.996	0.929	0.943	0.92	0.931
Other Shrub	0.99	0.797	0.829	0.776	0.802
Paddy field	0.996	0.915	0.949	0.888	0.917
Pasture	0.995	0.903	0.891	0.920	0.906
Pinus ECF	0.991	0.823	0.831	0.824	0.827
Pinus Shrub	0.999	0.782	0.643	1.000	0.783
Populus DBF	0.998	0.955	0.952	0.960	0.956
Pterocarya DBF	0.988	0.760	0.772	0.760	0.766

Preprints (www.preprints.org) | NOT PEER-REVIEWED | Posted: 28 December 2021 doi:10.20944/preprints202112.0443.v1

Quercus DBF	0.989	0.785	0.781	0.800	0.791
Quercus Shrub	0.990	0.799	0.862	0.752	0.803
Rhododendron Shrub	0.996	0.851	0.812	0.897	0.852
Robinia DBF	0.998	0.967	0.961	0.976	0.968
Salix DBF	0.994	0.879	0.893	0.872	0.883
Salix Shrub	0.994	0.879	0.868	0.896	0.882
Sasa Shrub	0.996	0.917	0.927	0.912	0.919
Thuja ECF	0.909	0.810	0.821	0.808	0.815
Thujopsis ECF	0.992	0.833	0.851	0.824	0.837
Tsuga ECF	0.992	0.845	0.821	0.880	0.849
Ulmus DBF	0.998	0.956	0.938	0.976	0.957
Upland field	0.996	0.918	0.920	0.920	0.920
Urban builtup	0.997	0.937	0.966	0.912	0.938
Water	1.000	0.992	0.992	0.992	0.992
Wetland Herb	0.998	0.954	0.975	0.936	0.955
Zanthoxylum DBF	0.997	0.904	0.886	0.925	0.905
Zelkova DBF	0.993	0.855	0.869	0.848	0.858

Table 4. Class-wise accuracy obtained for Kitakami site.

Classes	Accuracy	Kappa	F1-score	Recall	Precision
Abies ECF	0.995	0.932	0.941	0.929	0.935
Alnus DBF	0.987	0.811	0.852	0.786	0.818
Alpine Herb	0.998	0.964	0.962	0.970	0.966
Alpine Shrub	0.996	0.944	0.943	0.948	0.946
Bamboo EBF	1.000	0.850	0.755	0.974	0.851
Barren	0.993	0.899	0.918	0.888	0.903
Betula DBF	0.989	0.849	0.863	0.845	0.854
Carpinus DBF	0.996	0.946	0.924	0.974	0.948
Cryptomeria ECF	0.995	0.929	0.952	0.913	0.932
Fagus DBF	0.993	0.899	0.882	0.926	0.903
Fraxinus DBF	0.998	0.949	0.945	0.956	0.951
Juglans DBF	0.988	0.826	0.821	0.845	0.833
Larix DCF	0.995	0.927	0.935	0.924	0.930
Miscanthus Herb	0.991	0.868	0.895	0.852	0.873
Other Shrub	0.998	0.831	0.774	0.901	0.833
Paddy field	0.998	0.973	0.977	0.97	0.974
Pasture	0.998	0.971	0.971	0.974	0.972
Picea ECF	0.999	0.752	0.613	0.974	0.752
Pinus ECF	0.994	0.909	0.895	0.931	0.913
Pinus Shrub	1.000	0.913	0.840	1.000	0.913
Pterocarya DBF	0.992	0.885	0.895	0.883	0.889
Quercus DBF	0.988	0.820	0.877	0.782	0.827
Rhododendron Shrub	1.000	0.976	0.953	1.000	0.976
Robinia DBF	0.996	0.840	0.776	0.92	0.842
Salix DBF	0.993	0.885	0.913	0.865	0.889
Salix Shrub	0.997	0.894	0.855	0.94	0.895

Sasa Shrub	0.999	0.955	0.937	0.974	0.955
Thujopsis ECF	0.994	0.921	0.927	0.921	0.924
Tsuga ECF	0.996	0.947	0.952	0.946	0.949
Ulmus DBF	0.997	0.899	0.858	0.949	0.901
Upland field	0.994	0.907	0.925	0.896	0.910
Urban builtup	0.995	0.927	0.925	0.934	0.930
Water	0.999	0.979	0.978	0.982	0.980
Wetland Herb	0.996	0.937	0.941	0.938	0.939
Zelkova DBF	0.991	0.878	0.876	0.888	0.882
Zoysia Herb	0.999	0.792	0.670	0.969	0.792
Zoysia Herb	0.999	0.792	0.670	0.969	0.792

The classification accuracy matrices obtained for all study sites have been summarized in Table 5. The classification accuracy in terms of kappa coefficient varied from 87% in Oze site with 41 classes to 95% in Hakkoda site with 19 classes.

Table 5. Summary of classification accuracy metrics obtained for all sites.

Sites	Classes	Accuracy	Kappa	F1-score	Recall	Precision
Hakkoda	19	0.950	0.947	0.950	0.950	0.950
Zao	25	0.941	0.937	0.941	0.941	0.941
Oze	41	0.873	0.870	0.873	0.873	0.873
Shirakami	26	0.938	0.935	0.938	0.938	0.938
Kitakami	36	0.912	0.909	0.912	0.912	0.912

3.2. Land Cover and Plant Community Maps

The Land Cover and Plant Community Maps produced in this research have been shown in Figures 6-10. These maps demonstrate the extent and distribution of land cover and plant community types clearly for the study sites concerned.

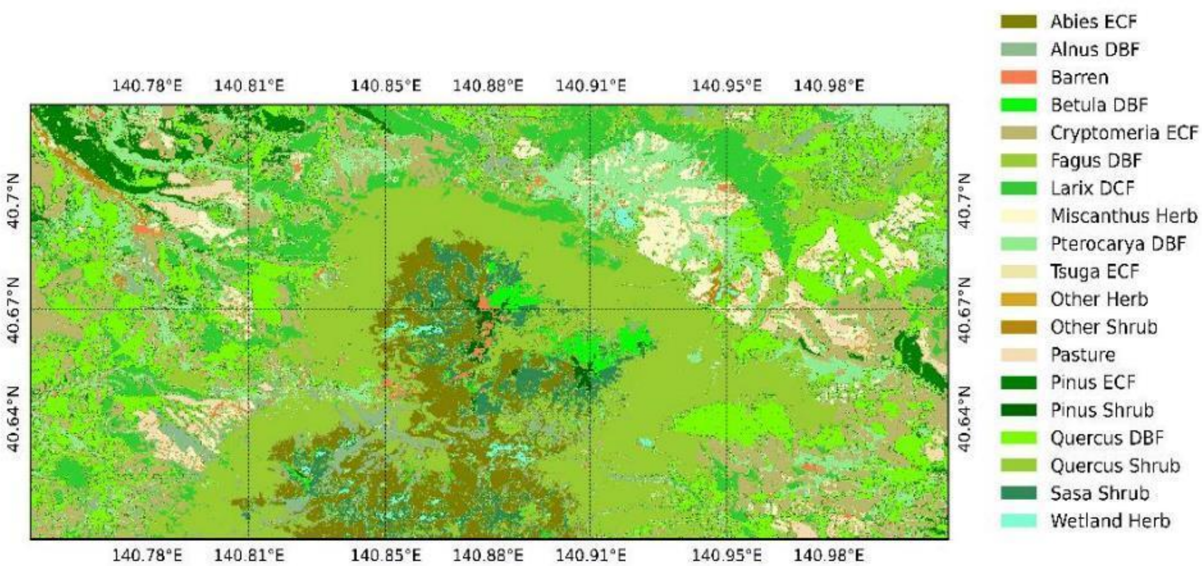

Figure 6. 19-class land cover and plant community map of Hakkoda site produced in the research.

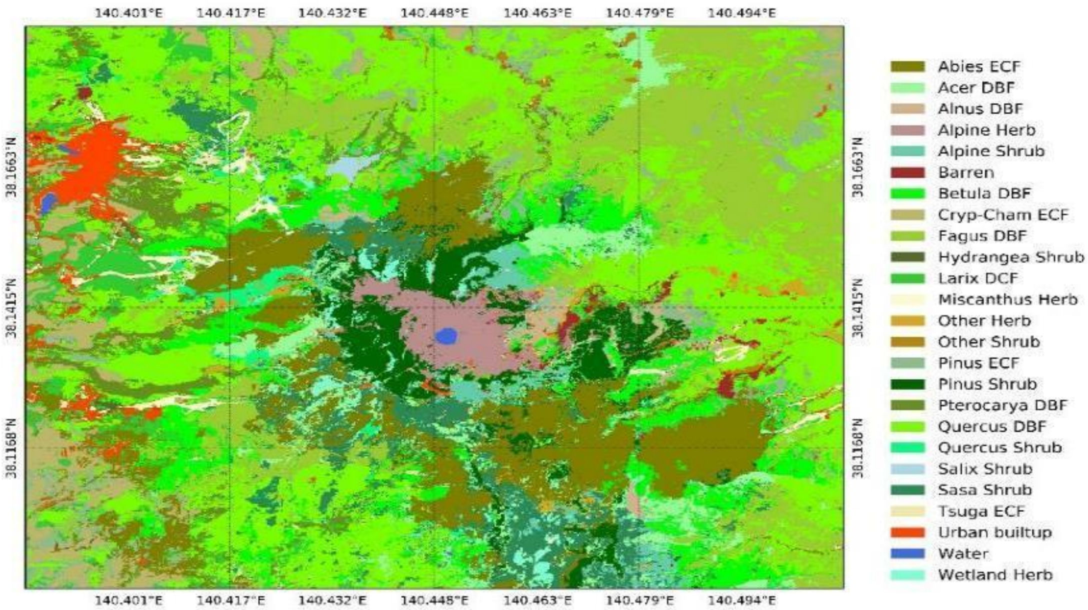

Figure 7. 25-class land cover and plant community map of Zao site produced in the research.

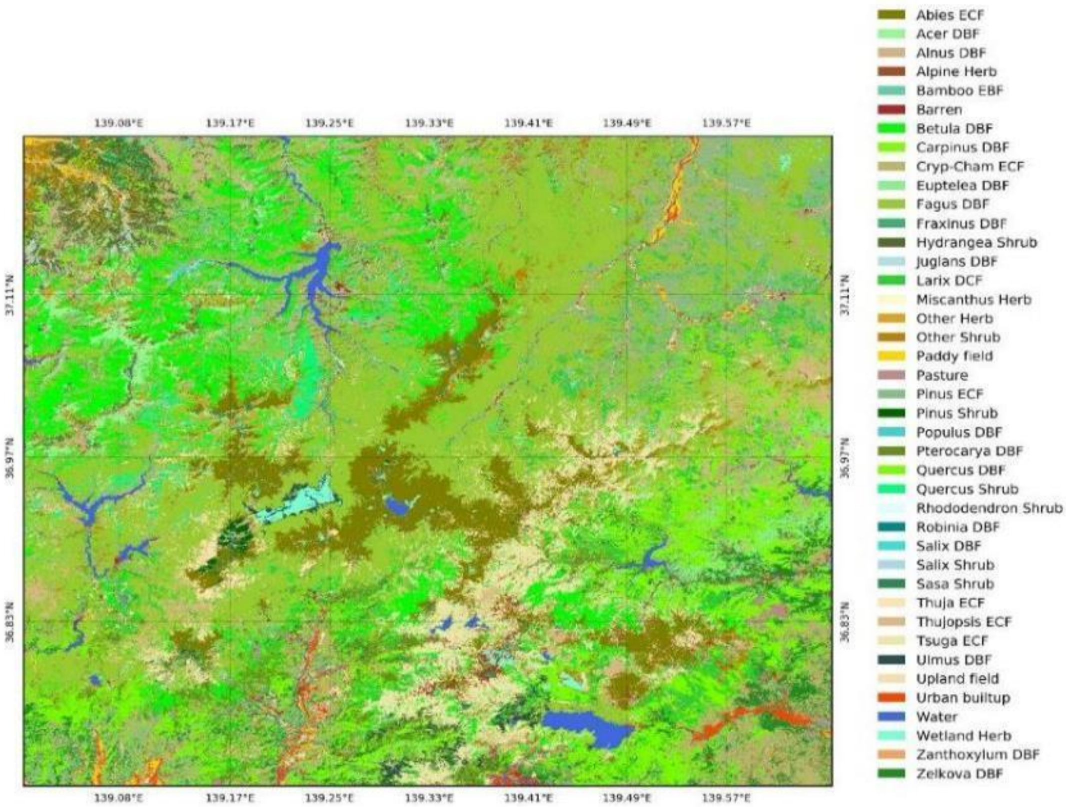

Figure 8. 41-class land cover and plant community map of Oze site produced in the research.

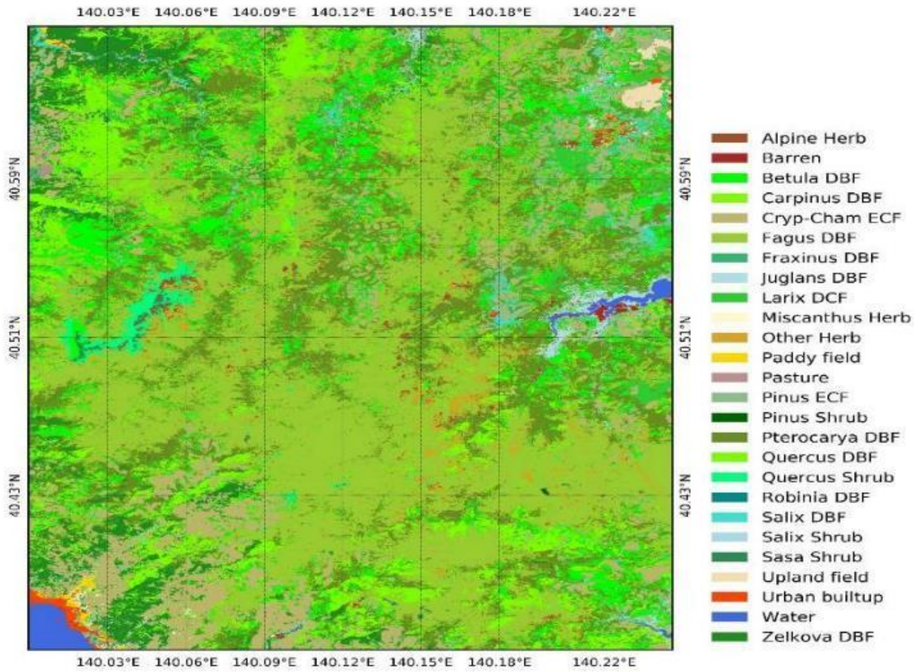

Figure 9. 26-class land cover and plant community map of Shirakami site produced in the research.

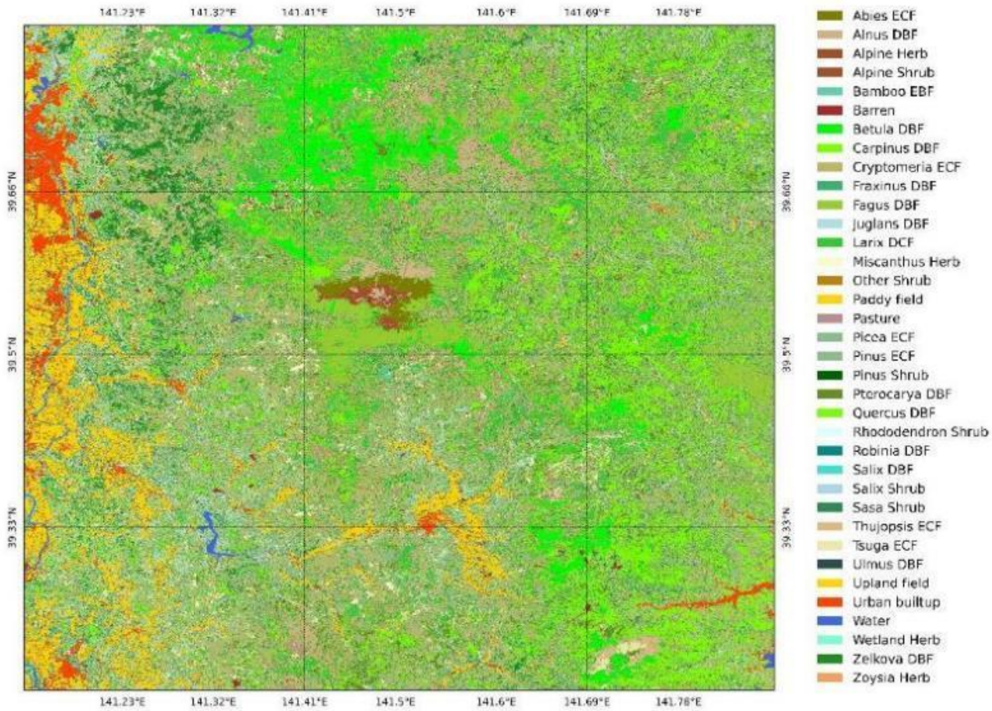

Figure 10. 36-class land cover and plant community map of Kitakami site produced in the research.

Preparation of ground truth data becomes very difficult, time-consuming, and expensive when the heterogeneity and complexity of plant community types increase. Even with the large amounts of high quality ground truth data, classification of satellite images becomes increasingly challenging as the number of classes increases. On the other hand, the characteristic species based phyto-sociological classes (Poore, 1955; Whittaker, 1980; Miyawaki and Fujiwara, 1988) delineated by nationwide vegetation survey is out from automated digital mapping approach as remote sensing signals are mostly governed by physical interactions of dominant species rather than characteristic species. Therefore, a right and effective organization of plant communities is essential for operational and broad-scale mapping. In line with this, the Genus-Physiognomy-Ecosystem (GPE) system, developed by Sharma, 2021 for the classification of plant communities from the perspective of satellite remote sensing, was extended in this research for operational mapping of land cover and plant community types collectively.

4. Conclusions

In this research, we presented operational mapping of land cover and plant community types in five study sites in a temperate region in Japan by utilizing multi-spectral and multi-temporal Sentinel-2. Machine learning based accuracy analysis showed potential of the Sentinel-2 images for the mapping of land cover and plant community types by adopting Genus-Physiognomy-Ecosystem (GPE) system as the kappa coefficient varied from 87% (41 classes in Oze site) to 95% (19 classes in Hakkoda site). Still, some misclassifications were detected in some classes such as Betula DBF, Alnus DBF, Fagus DBF, Quercus DBF, Picea ECF, Hydrangea Shrub, and Zoysia Herb particularly in sites associated with many classes. Further increase in the temporal resolution of Sentinel-2 mission satellites images with future launches of Sentinel-2C and 2D satellites is highly expected for improving the classification accuracy of plant communities. Future plan is to expand this methodology for seamless mapping of plant communities in the same region by further increasing the ground truth data.

Author Contributions: R. Sharma conceptualized the research, performed the research, and wrote the manuscript. H. Hirayama assisted in data processing and analysis. M. Yasuda and I. Asai assisted in the organization and collection of groundtruth data. K. Hara supervised the research. All authors have read and agreed to the published version of the manuscript.

Funding: The field data was supported by the commissioned research of the Ministry of the Environment, Center for Biodiversity and Asia Air Survey Co., Ltd. This research was partially supported by JSPS Grant-in-Aid for Scientific Research (JP19H04320).

Conflicts of Interest: The authors declare no conflict of interest.

References

1. Bredenkamp, G.; Chytrý, M.; Fischer, H.S.; Neuhäuslová, Z.; van der Maarel, E. Vegetation Mapping: Theory, Methods and Case Studies: Introduction. *Applied Vegetation Science* **1998**, *1*, 162–164.
2. Drusch, M.; Del Bello, U.; Carlier, S.; Colin, O.; Fernandez, V.; Gascon, F.; Hoersch, B.; Isola, C.; Laberinti, P.; Martimort, P.; et al. Sentinel-2: ESA's Optical High-Resolution Mission for GMES Operational Services. *Remote Sensing of Environment* **2012**, *120*, 25–36, doi:10.1016/j.rse.2011.11.026.
3. Falkowski, M.J.; Gessler, P.E.; Morgan, P.; Hudak, A.T.; Smith, A.M.S. Characterizing and Mapping Forest Fire Fuels Using ASTER Imagery and Gradient Modeling. *Forest Ecology and Management* **2005**, *217*, 129–146, doi:10.1016/j.foreco.2005.06.013.
4. Gitelson, A.A.; Gritz †, Y.; Merzlyak, M.N. Relationships between Leaf Chlorophyll Content and Spectral Reflectance and Algorithms for Non-Destructive Chlorophyll Assessment in Higher Plant Leaves. *Journal of Plant Physiology* **2003**, *160*, 271–282, doi:10.1078/0176-1617-00887.
5. Gitelson, A.A.; Kaufman, Y.J.; Merzlyak, M.N. Use of a Green Channel in Remote Sensing of Global Vegetation from EOS-MODIS. *Remote Sensing of Environment* **1996**, *58*, 289–298, doi:10.1016/S0034-4257(96)00072-7.
6. Hengl, T.; Walsh, M.G.; Sanderman, J.; Wheeler, I.; Harrison, S.P.; Prentice, I.C. Global Mapping of Potential Natural Vegetation: An Assessment of Machine Learning Algorithms for Estimating Land Potential. *PeerJ* **2018**, *6*, e5457, doi:10.7717/peerj.5457.
7. Himiyama, Y. Land Use/Cover Changes in Japan: From the Past to the Future. *Hydrological Processes* **1998**, *12*, 1995–2001, doi:10.1002/(SICI)1099-1085(19981030)12:13/14<1995::AID-HYP714>3.0.CO;2-C.
8. Hioki, Y. Issues of Nation -Wide Actual Vegetation Maps from the Aspect for Application. *Landscape Ecology and Management* **2007**, *11*, 107–112, doi:10.5738/jale.11.107.

9. Huete, A.; Didan, K.; Miura, T.; Rodriguez, E.P.; Gao, X.; Ferreira, L.G. Overview of the Radiometric and Biophysical Performance of the MODIS Vegetation Indices. *Remote Sensing of Environment* **2002**, *83*, 195–213, doi:10.1016/S0034-4257(02)00096-2.
10. Huete, A.R. A Soil-Adjusted Vegetation Index (SAVI). *Remote Sensing of Environment* **1988**, *25*, 295–309, doi:10.1016/0034-4257(88)90106-X.
11. Kaufman, Y.J.; Tanre, D. Atmospherically Resistant Vegetation Index (ARVI) for EOS-MODIS. *IEEE Trans. Geosci. Remote Sensing* **1992**, *30*, 261–270, doi:10.1109/36.134076.
12. Louhaichi, M.; Borman, M.M.; Johnson, D.E. Spatially Located Platform and Aerial Photography for Documentation of Grazing Impacts on Wheat. *Geocarto International* **2001**, *16*, 65–70, doi:10.1080/10106040108542184.
13. Miyawaki, A. A Vegetation-Ecological View of the Japanese Archipelago. *Bulletin of the Institute of Environmental Science and Technology* **1984**, *11*, 85–101.
14. Miyawaki, A. Typen von Vegetationskarten Und Ihre Anwendung Fur Die Beurteilung Des Standortes. *Map, Journal of the Japan Cartographers Association* **1968**, *6*, 1–9.
15. Miyawaki, A.; Fujiwara, K. Vegetation Mapping in Japan. In *Vegetation mapping*; Küchler, A.W., Zonneveld, I.S., Eds.; Springer Netherlands: Dordrecht, 1988; pp. 427–441 ISBN 978-94-010-7885-6.
16. MoE Nature Conservation Bureau, Ministry of the Environment of Japan and Asia Air Survey Co., Ltd. The 5th National Survey on the Natural Environment (Vegetation Survey) Report 1999.
17. Murakami T.; Mochizuki S. Vegetation mapping using remotely sensed imagery 2014.
18. Numata, M.; Miyawaki, A.; Itow, D. Natural and Semi-Natural Vegetation in Japan. *Blumea* **1972**, *20*, 435–496.
19. Ohno, K. Applications of a Phytosociological Vegetation Map and Its Role for Development with Landscape Ecology. *Landscape Ecology and Management* **2006**, *11*, 39–52, doi:10.5738/jale.11.39.
20. Penuelas, J.; Frederic, B.; Filella, I. Semi-Empirical Indices to Assess Carotenoids/Chlorophyll-a Ratio from Leaf Spectral Reflectance. *Photosynthetica* **1995**, *31*, 221–230.
21. Poore, M.E.D. The Use of Phytosociological Methods in Ecological Investigations: I. The Braun-Blanquet System. *The Journal of Ecology* **1955**, *43*, 226, doi:10.2307/2257132.
22. Qi, J.; Chehbouni, A.; Huete, A.R.; Kerr, Y.H.; Sorooshian, S. A Modified Soil Adjusted Vegetation Index. *Remote Sensing of Environment* **1994**, *48*, 119–126, doi:10.1016/0034-4257(94)90134-1.
23. Rondeaux, G.; Steven, M.; Baret, F. Optimization of Soil-Adjusted Vegetation Indices. *Remote Sensing of Environment* **1996**, *55*, 95–107, doi:10.1016/0034-4257(95)00186-7.
24. Rouse, J.W.; Haas, R.H.; Schell, J.A.; Deering, D.W. Monitoring Vegetation Systems in the Great Plains with ERTS. *NASA special publication* **1974**, *351*, 309.
25. Sharma, R.C. Genus-Physiognomy-Ecosystem (GPE) System for Satellite-Based Classification of Plant Communities. *Ecologies* **2021**, *2*, 203–213, doi:10.3390/ecologies2020012.
26. Sims, D.A.; Gamon, J.A. Relationships between Leaf Pigment Content and Spectral Reflectance across a Wide Range of Species, Leaf Structures and Developmental Stages. *Remote Sensing of Environment* **2002**, *81*, 337–354, doi:10.1016/S0034-4257(02)00010-X.
27. Su, Y.; Guo, Q.; Hu, T.; Guan, H.; Jin, S.; An, S.; Chen, X.; Guo, K.; Hao, Z.; Hu, Y.; et al. An Updated Vegetation Map of China (1:1000000). *Science Bulletin* **2020**, *65*, 1125–1136, doi:10.1016/j.scib.2020.04.004.
28. Whittaker, R.H. *Classification of Plant Communities*; Springer Netherlands: Dordrecht, 1980; ISBN 978-94-009-9183-5.
29. Wulder, M.A.; Coops, N.C.; Roy, D.P.; White, J.C.; Hermosilla, T. Land Cover 2.0. *International Journal of Remote Sensing* **2018**, *39*, 4254–4284, doi:10.1080/01431161.2018.1452075.